

Dynamics of Localization Phenomena for Hardcore Bosons in Optical Lattices

Birger Horstmann,^{1,2} J. Ignacio Cirac,¹ and Tommaso Roscilde¹

¹*Max-Planck-Institut für Quantenoptik, Hans-Kopfermann-Straße 1, 85748 Garching, Germany*

²*Institut für Theoretische Physik, Friedrich-Schiller-Universität, Max-Wien-Platz 1, 07743 Jena, Germany*

We investigate the behavior of ultracold bosons in optical lattices with a disorder potential generated via a secondary species frozen in random configurations. The statistics of disorder is associated with the physical state in which the secondary species is prepared. The resulting random potential, albeit displaying algebraic correlations, is found to lead to localization of all single-particle states. We then investigate the real-time dynamics of localization for a hardcore gas of mobile bosons which are brought into sudden interaction with the random potential. Regardless of their initial state and for any disorder strength, the mobile particles are found to reach a steady state characterized by exponentially decaying off-diagonal correlations and by the absence of quasi-condensation; when the mobile particles are initially confined in a tight trap and then released in the disorder potential, their expansion is stopped and the steady state is exponentially localized in real space, clearly revealing Anderson localization.

PACS numbers: 03.75.Lm, 03.75.Mn, 64.60.My, 72.15.Rn

I. INTRODUCTION

The adiabatic loading of ultracold atoms and molecules in optical lattices represents a formidable opportunity to engineer strongly correlated states of quantum many-body systems with unprecedented control^{1,2,3,4}. On the one hand, known fundamental models for the physics of solid state systems can be literally implemented in optical lattices^{5,6}, and the experimental detection of their ground state or thermal equilibrium properties has the potential of responding to the lack of theoretical results due to fundamental limitations in the calculations, as those generally reported in fermionic systems or in frustrated quantum magnets. On the other hand, optical lattice systems offer the further advantage of controlling the Hamiltonian parameters in real time, and this enriches the range of correlated phases that can be implemented, if one can guide the evolution of the system towards an off-equilibrium state which is not necessarily an eigenstate of a known Hamiltonian.

An intense activity has recently been focused on the experimental implementation of disorder potentials in systems of trapped ultracold bosons, both experimentally^{7,8,9,10,11,12} and theoretically^{13,14,15,16,17,18,19,20,21,22,23}. The introduction of tunable randomness in the system offers the possibility of realizing Anderson localization of coherent matter waves of weakly interacting bosons^{8,9,10} and the opportunity of investigating the interplay between strong localization and strong interaction, *e.g.* in a deep optical lattice¹¹. The fundamental model describing this rich phenomenology in presence of a lattice is the Bose-Hubbard model in a random potential²⁴, where, beside the conventional Mott insulating and superfluid phases, a Bose-glass phase appears, either associated with the fragmentation of weakly repulsive bosons into exponentially localized states, or with the localization of collective gapless modes for strong repulsion.

The disorder potential has so far been realized opti-

cally, either through laser speckles^{7,8,9,10} with or without an optical lattice, or, in optical lattices, through a secondary incommensurate standing wave¹¹. In the case of speckles, the typical length scale associated with the disorder potential is quite extended with respect to the correlation length of the bosons, so that classical trapping rather than quantum localization is responsible for the observed suppression of transport properties^{12,25}. On the other hand, the incommensurate superlattice of Ref. 11 realizes a potential which is strongly fluctuating over the distance of a few lattice sites, but its *pseudo*-disordered nature requires to take also into account gapped insulating phases at incommensurate fillings, competing with the Bose glass²⁶.

An alternative proposal to create disorder in optical lattices involves the repulsive interaction with a secondary species of particles^{27,28}. If the two species correspond to two different hyperfine states of the atoms, the use of state-dependent optical lattices^{29,30,31} allows one to first decouple the two species, and then to selectively suppress the hopping of one of them, freezing it in a given quantum state $|\Phi^f\rangle$.

If the two species are subsequently brought into interaction, the mobile one evolves in a quantum superposition of all possible realizations of the random potential associated with the Fock components of $|\Phi^f\rangle$, and expectation values over the evolved state are therefore automatically averaged over the disorder distribution²⁸. In this proposal not only is the disorder potential strongly fluctuating over the length scale of a few lattice sites, but in principle one can also vary its statistics by preparing the frozen bosons in different states $|\Phi^f\rangle$.

In this paper we investigate the above proposal in detail in the exactly solvable case of a one-dimensional gas of hardcore bosons on a lattice^{32,33}. We consider both species of bosons (the mobile one and the frozen one) to be hardcore repulsive, which is not only experimentally feasible^{33,34}, but it has three fundamental theoretical advantages: 1) the state $|\Phi^f\rangle$ of the frozen

bosons can be obtained exactly from the Hamiltonian of the system before freezing, and disorder averaging can therefore be accurately performed; 2) Jordan-Wigner diagonalization³² allows to calculate the exact real-time evolution of the mobile particles^{35,36,37} after they are brought into interaction with the frozen ones; 3) and, most importantly from a conceptual point of view, localization phenomena of hardcore bosons are perfectly understood in terms of Anderson localization of non-interacting fermions. While the observation of localization for interacting bosons is limited by screening of the disorder potential and the reduction of the healing length due to the interaction^{7,8,9,10,11,12}, many-body effects enter the system of non-interacting fermions only through Fermi statistics.

In particular we focus on the case in which the frozen bosons are initially prepared in the superfluid ground state $|\Phi^f\rangle$ of the hardcore-boson Hamiltonian at *half* filling with periodic boundary conditions. The resulting disorder potential has the structure of a bimodal random on-site energy, with algebraically decaying correlations, but also with a very rich Fourier spectrum dominated by short-wavelength components. Most importantly, such a potential is found to lead to Anderson localization of all single-particle eigenstates (apart from possibly a set of zero measure) as expected for uncorrelated disorder^{38,39}. The evolution of the mobile bosons in such a potential is found to invariably lead to a disordered steady state with exponentially decaying correlations and absence of quasi-condensation for a wide variety of realistic initial conditions. In particular phenomena of quasi-condensation in finite-momentum states³⁶ and fermionization³⁷, reported upon expansion of the hardcore bosons from a Mott-insulating state and a superfluid state respectively, are completely washed out by the disorder potential. Hence we can conclude that this setup allows for a robust implementation of a localized state as the off-equilibrium steady state of the system evolution.

This paper is structured as follows: Section II describes the system of two bosonic species, the exact diagonalization method for the study of real-time evolution, the Monte Carlo sampling of the disorder distribution, and the main features of the random potential; Section III is devoted to the study of localization of the single-particle eigenstates in the random potential; Section IV investigates the evolution of the mobile bosons after interaction with the frozen ones when both species are prepared on a ring; finally, Section V is dedicated to the study of the expansion of the mobile bosons in the random potential, starting from different initial confined states.

II. SYSTEM AND METHOD

In this section we present the system of two bosonic species which is used to study the effect of a disorder potential (subsection II A). We then briefly describe the numerical procedure to exactly treat the equilibrium and

out-of-equilibrium properties of the system (subsection II B), and the sampling of the disorder distribution (subsection II C). Finally, we examine the nature of the correlations in the disorder potential created by a frozen species of hardcore bosons in subsection II D.

A. Hamiltonian Dynamics

The full system of two trapped interacting bosonic species in a one-dimensional optical lattice is described by the Hamiltonian

$$\mathcal{H} = \mathcal{H}_0 + \mathcal{H}_f + \mathcal{H}_{\text{int}}, \quad (1)$$

where \mathcal{H}_0 is the Hamiltonian of the bosons which will remain mobile,

$$\begin{aligned} \mathcal{H}_0 = & - J \sum_{i=1}^L (a_i^\dagger a_{i+1} + \text{h.c.}) \\ & + \sum_{i=1}^L \left[\frac{U}{2} n_i (n_i - 1) + V (i - i_0)^2 n_i \right], \end{aligned} \quad (2)$$

\mathcal{H}_f is the Hamiltonian for the bosons to be frozen,

$$\begin{aligned} \mathcal{H}_f = & - J^f \sum_{i=1}^L (a_i^{f\dagger} a_{i+1}^f + \text{h.c.}) \\ & + \sum_{i=1}^L \left[\frac{U^f}{2} n_i^f (n_i^f - 1) + V^f (i - i_0)^2 n_i^f \right], \end{aligned} \quad (3)$$

and \mathcal{H}_{int} is the interaction Hamiltonian

$$\mathcal{H}_{\text{int}} = W \sum_{i=1}^L n_i n_i^f. \quad (4)$$

Here L is the number of sites of the system, a_i^\dagger and a_i are boson creation and annihilation operators and $n_i = a_i^\dagger a_i$ is the number operator for site i . Symbols with the superscript f are the corresponding operators for the frozen bosons that create the disorder potential. In Eqs. (2),(3) we also consider the possibility of both species being confined by a parabolic trap with different trapping strengths V, V^f .

At times $t < 0$ the two species of bosons are not interacting with each other ($W = 0$), and they are prepared in the factorized ground state $|\Psi\rangle = |\Phi^f\rangle \otimes |\Phi\rangle$ of their respective Hamiltonian with fixed numbers of particles N and N^f . The ground state $|\Phi^f\rangle$ of the frozen particles can be decomposed in the Fock basis

$$|\Phi^f\rangle = \sum_{\{n_i^f\}} c(\{n_i^f\}) |\{n_i^f\}\rangle, \quad (5)$$

where the sum extends over all Fock states,

$$\{n_i^f\} = \left(n_1^f, n_2^f, \dots, n_L^f : \sum_{i=1}^L n_i^f = N^f \right). \quad (6)$$

At some time $t \leq 0$ the frozen bosons are made immobile ($J^f = 0$), and subsequently at $t = 0$ the interaction between the two species is turned on ($W > 0$). Furthermore, releasing the mobile bosons from their trap ($V = 0$) allows us to study their expansion properties.

The time evolution of the initially prepared state for $t > 0$ is described by

$$\begin{aligned} |\Psi(t)\rangle &= e^{-i\mathcal{H}t} \sum_{\{n_i^f\}} c(\{n_i^f\}) |\{n_i^f\}\rangle \otimes |\Phi\rangle \\ &= \sum_{\{n_i^f\}} c(\{n_i^f, t\}) |\{n_i^f\}\rangle \otimes |\Phi(t, \{n_i^f\})\rangle, \end{aligned} \quad (7)$$

where the coefficients $c(\{n_i^f, t\}) = e^{-i\phi(\{n_i^f\})t} c(\{n_i^f\})$ have acquired a phase factor which will become irrelevant, and the state

$$|\Phi(t, \{n_i^f\})\rangle = \exp\{-i[\mathcal{H}_0 + \mathcal{H}_{int}(\{n_i^f\})]t\} |\Phi\rangle \quad (8)$$

represents the time evolution of the initial state of the mobile bosons interacting with a single Fock state $|\{n_i^f\}\rangle$ of the frozen bosons, which determines the static external potential. We have used the property that, for $J^f = 0$, $[\mathcal{H}_f, \mathcal{H}_0 + \mathcal{H}_{int}] = 0$.

Hence, equation (7) describes the parallel time evolution of the mobile bosons in a *quantum superposition* of different realizations of the disorder potential $V_i = V n_i^f$, each appearing with a probability $P(\{n_i^f\}) = |c(\{n_i^f\})|^2$. Remarkably, the time evolution of the expectation value of an operator A acting only on the mobile bosons is automatically averaged over the disorder statistics²⁸:

$$\begin{aligned} \langle \Psi(t) | A | \Psi(t) \rangle &= \\ &= \sum_{\{n_i^f\}} |c(\{n_i^f\})|^2 \langle \Phi(t, \{n_i^f\}) | A | \Phi(t, \{n_i^f\}) \rangle. \end{aligned} \quad (9)$$

B. Hardcore limit and Jordan-Wigner Transformation

From here onwards we will restrict ourselves to the exactly solvable case of *hardcore* bosons, obtained in the limit $U, U^f \rightarrow \infty$ for filling smaller than or equal to one. It is convenient to incorporate the hardcore constraint directly in the operator algebra, passing to hardcore boson operators which *anticommute* on the same site, $\{a_i, a_i^\dagger\} = 1$, $\{a_i^{(\dagger)}, a_i^{(\dagger)}\} = 0$, and $\{a_i^f, a_i^{f\dagger}\} = 1$, $\{a_i^{f(\dagger)}, a_i^{f(\dagger)}\} = 0$.

Making use of the Jordan-Wigner transformation³²,

$$a_i^\dagger = f_i^\dagger \prod_{k=1}^{i-1} e^{-i\pi f_k^\dagger f_k}, \quad a_i = \prod_{k=1}^{i-1} e^{i\pi f_k^\dagger f_k} f_i, \quad (10)$$

one can map the hardcore bosons operators onto spinless fermion operators f_i^\dagger and f_i , obeying the same Hamiltonian as the bosonic one, apart from a boundary term depending on the number of particles in the case of periodic/antiperiodic boundary conditions. The fermionic problem is exactly solvable, and its eigenstates can be written in the following form

$$|\Phi\rangle = \prod_{m=1}^N \sum_{n=1}^L P_{nm} f_n^\dagger |0\rangle, \quad (11)$$

where the N columns of the matrix $P_{nm} = \{\mathbf{P}\}_{nm}$ represent the first N single-particle eigenstates. Following the recipe of Ref. 35, from the matrix P_{nm} one can efficiently calculate the one-particle density matrix (OPDM)

$$\rho_{ij} = \langle a_i^\dagger a_j \rangle, \quad (12)$$

and hence the momentum distribution

$$\langle n_k \rangle = \frac{1}{L} \sum_{m,n=1}^L e^{-ik(m-n)} \langle a_m^\dagger a_n \rangle \quad (13)$$

which represents a fundamental observable in trapped atomic systems. At a more fundamental level, the knowledge of the eigenvalues λ_η of the OPDM, associated to eigenvectors ϕ_η^η also known as natural orbitals (NO), allows one to rigorously study condensation phenomena through the scaling of the maximum eigenvalue λ_0 with the particle number^{35,40}. In absence of an external potential the OPDM of the hardcore bosons decays algebraically as $\rho_{ij} \sim |i-j|^{-\alpha}$, where $\alpha = 0.5$, signaling off-diagonal quasi-long-range order in the system⁴¹. Correspondingly the occupation of the $k = 0$ momentum state, which coincides with the natural orbital with largest eigenvalue for a translationally invariant system, scales as $n_{k=0} \sim \sqrt{N}$ with the particle number N for any fixed density $n = N/L < 1$, namely it exhibits *quasi-condensation*. Remarkably, quasi-long-range order and quasi-condensation (in the form of a \sqrt{N} scaling of the largest eigenvalue λ_0 of the OPDM) survive also in presence of a trapping potential $V(i-i_0)^a$ when the particle number is increased and correspondingly the trap strength V is decreased so that the characteristic density in the trap

$$\tilde{\rho} = N \left(\frac{V}{J} \right)^{1/a}, \quad (14)$$

is kept constant and smaller than a critical value ρ_c (≈ 2.6 for $a = 2$) to avoid formation of a Mott plateau in the trap center³⁵.

Finally, the exact solution of the fermionic Hamiltonian allows one to calculate the real-time evolution of the fermionic wavefunction, and in particular of the \mathbf{P} matrix as

$$\mathbf{P}(t) = e^{-i\mathbf{H}t}\mathbf{P} \quad (15)$$

with the single-particle time evolution operator given by

$$(e^{-i\mathbf{H}t})_{ij} = \langle 0 | f_i e^{-i\mathbf{H}t} f_j^\dagger | 0 \rangle. \quad (16)$$

Making use of this approach, Refs. 36,37 have shown that quasi-condensation is a robust feature of the system after expansion starting from an initially trapped quasi-condensed state, and it is even dynamically recovered when the initial state before expansion is a fully incoherent Mott insulator state.

C. Disorder Averaging

Eq. (9) shows that, ideally, the unitary evolution of the system explores all possible realizations of the disordered potential at once. Numerical calculations based on a matrix-product-state representation of the system state also enjoy this feature of "quantum parallelism" of the Hamiltonian evolution²⁸ by treating the disorder potential as a quantum variable in the system. In this paper we use the more traditional approach of exactly calculating the ground-state properties and the Hamiltonian evolution of hardcore bosons for a single realization of disorder at a time, averaging then over the disorder distribution through Monte Carlo importance sampling. Accepting the overhead of disorder averaging, this approach has the advantage that, unlike the method of Ref. 28, the time evolution is exact for arbitrarily long times.

According to Eq. (9), the weights of the disorder configurations are defined by the coefficients of the Fock-state decomposition for the initial state of the frozen bosons through $P(\{n_i^f\}) = |c(\{n_i^f\})|^2$. Introducing the bosonic Fock state

$$|\{n_i^f\}\rangle = a_{i_1}^\dagger a_{i_2}^\dagger \dots a_{i_{N^f}}^\dagger |0\rangle \quad (17)$$

and the $N^f \times L$ matrix $Q_{nm} = \{\mathbf{Q}\}_{nm} = \delta_{i_n, m}$, after some algebra we get

$$c(\{n_i^f\}) = \langle \{n_i^f\} | \Phi_f \rangle = \det(\mathbf{Q}^\dagger \mathbf{P}). \quad (18)$$

The energy eigenstates of noninteracting fermions with periodic boundary conditions, contained in the columns of the \mathbf{P} matrix, are given by plain waves. Thus it can be shown that the Slater determinant of Eq. (18) is a Vandermonde determinant, which can be evaluated analytically. The disorder weights finally become

$$|c(\{n_i^f\})|^2 = \frac{1}{L^{N^f}} \prod_{1 \leq n < m \leq N^f} \sin^2 \left[\frac{\pi}{L} (i_n - i_m) \right]. \quad (19)$$

Throughout the paper we will compare the effect of the disorder potential generated by the frozen superfluid state of N^f bosons with that of the potential generated by N^f *fully uncorrelated* frozen bosons⁴³, with the flat distribution

$$|c(\{n_i^f\})|^2 = (N^f!(L - N^f)!)/L!. \quad (20)$$

Even when equipped with the exact statistics of disorder as in Eqs. (19) and (20), it is generally hopeless to fully average the results of any calculation on the $L/(N^f!(L - N^f)!)$ disorder configurations. Hence we opt for Monte Carlo importance sampling, where starting from an initially chosen random configuration $|\{n_i^f\}\rangle$, we propose a new one $|\{n_i^f\}'\rangle$ (e.g. by swapping the occupation of two sites) and accept it with Metropolis probability $p = \min(|c(\{n_i^f\}')|^2/|c(\{n_i^f\})|^2, 1)$. The real-space properties are typically averaged over 10^5 disorder realizations, obtained one from the other by updating $O(L)$ sites, while the OPDM is averaged over 10^2 realizations (due to the computational overhead of the OPDM calculation). This provides full convergence of the disorder-averaged quantities.

D. Characteristics of Disorder

A fundamental figure of merit for the proposed setup to introduce disorder in optical lattices is represented by the correlation properties of the disorder potential generated by the frozen particles. As discussed in the introduction, the aspect of correlations represents one of the main weaknesses of the optical implementation of disorder through laser speckles¹². In particular, we focus on the density-density correlation function

$$C_r(|\Phi^f\rangle) = \frac{\frac{1}{L} \sum_{i=1}^L \langle (n_i^f - n^f)(n_{i+r}^f - n^f) \rangle}{\frac{1}{L} \sum_{i=1}^L \langle (n_i^f - n^f)^2 \rangle}, \quad (21)$$

where $n^f = \langle n_i^f \rangle = N^f/L$. This correlation function for the frozen hardcore bosons is identical to the one for the corresponding fermions, and can be calculated exactly in the homogeneous system ($V^f = 0$) with periodic boundary conditions; for $N^f < L$, namely in the superfluid state of hardcore bosons,

$$C_r(|\Phi^f\rangle) = \begin{cases} 1 & \text{for } r = 0 \\ -[N^f(L - N^f)]^{-1} \frac{\sin^2(\pi \frac{N^f r}{L})}{\sin^2(\pi \frac{r}{L})} & \text{for } r \geq 1 \end{cases} \quad (22)$$

Hence, in the limit $r \ll L$ (which is always satisfied in the thermodynamic limit) the correlator decays algebraically like $C_r(|\Phi^f\rangle) \sim r^{-2}$ with a superimposed oscillation at twice the Fermi wavevector $k_F = \pi n^f$. The negative values of the correlator can be understood as resulting from

an effective long-range repulsion between the hardcore bosons due to the kinetic energy, which enjoys as much free space around each boson as possible.

From Eq. (22) we deduce that the disorder potential created by the frozen bosons has slowly decaying correlations. Nonetheless it has fast oscillations on short distances, which are captured by the structure factor, namely the Fourier transform of the correlator:

$$C_k = \frac{1}{L} \sum_{r=0}^{L-1} C_r \cos(kr). \quad (23)$$

This function can be evaluated to give for $k \in [-\pi, \pi]$ and $n^f \leq 0.5$

$$C_k = \begin{cases} \frac{1}{L(1-n^f)} \cdot \frac{|k|}{2k_F} & \text{for } |k| \leq 2k_F \\ \frac{1}{L(1-n^f)} & \text{for } 2k_F \leq |k| \leq \pi. \end{cases} \quad (24)$$

The expression for $n^f > 0.5$ follows from particle-hole symmetry. The corresponding functions for an uncorrelated random potential generated by randomly displayed frozen particles are $C_r = \delta_{r0}$ and $C_k = 1/L$. We observe that the Fourier spectrum of the frozen-boson potential is extremely broad, and it has a flat maximum for $k \geq k_F$, reflecting the short wavelength oscillations of the potential. Hence we are in presence of a correlated but strongly fluctuating potential. In the following section we will see that such a potential generally leads to Anderson localization of all single-particle states and to the suppression of quasi-condensation at all fillings. Throughout the rest of the paper, we will take the case of half-filling for the frozen bosons, $N^f = L/2$.

III. GROUND-STATE PROPERTIES

In this section we investigate the properties of the eigenstates of the Hamiltonian $\mathcal{H}_0 + \mathcal{H}_{int}$ (see equations (2) and (4)) for the mobile bosons moving in the potential created by the frozen bosons. Here we consider an homogeneous system ($V = V^f = 0$) with periodic boundary conditions for both species of bosons. We start with an analysis of the localization properties in real space and continue with an analysis of coherence in momentum space.

We investigate the localization properties in the frozen-boson potential through the *participation ratio* (PR) defined as

$$\text{PR}(|\Phi\rangle) = \frac{\left(\sum_{i=1}^L \langle n_i \rangle\right)^2}{\sum_{i=1}^L \langle n_i \rangle^2}, \quad (25)$$

where $\langle n_i \rangle$ is the average particle density on site i . In the case of a rectangular density profile the participation ratio gives the support of the density profile, for exponentially localized states it is proportional to the decay

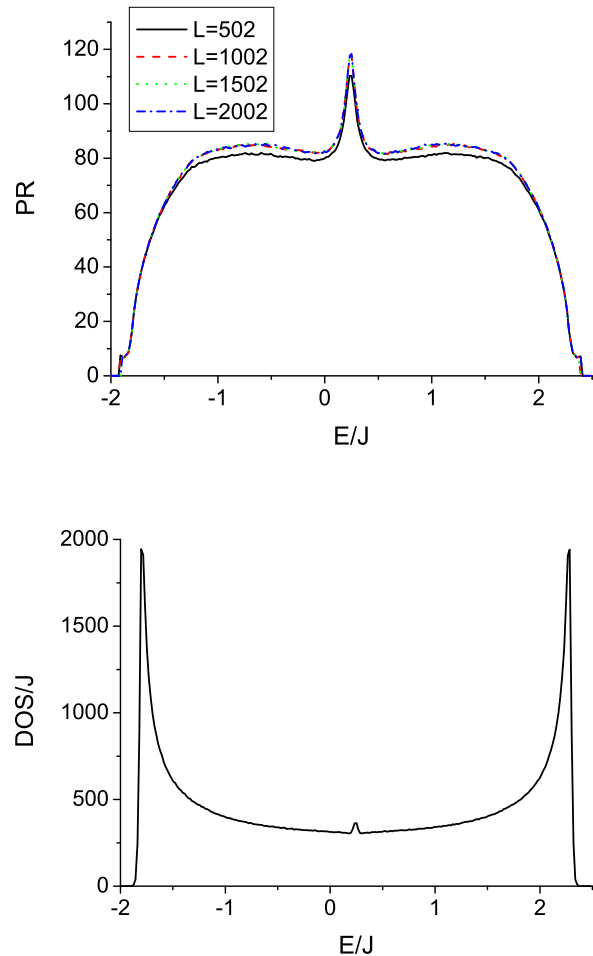


FIG. 1: (Color online) Average participation ratio (*upper plot*) and density of states (*lower plot*) of the single-particle energy eigenstates in the correlated random potential created by frozen bosons with disorder strength $W = 0.5J$. The density of states is calculated for a system size $L = 2002$.

length of the wavefunction, and for a Gaussian-shaped density profile it is proportional to its standard deviation.

The average PR of single particle eigenstates in the potential created by a half-filled system of frozen bosons at $W = 0.5J$ is shown in the upper panel of Fig. 1 as a function of energy, for various system sizes. The PR essentially becomes size independent for $L \geq 1000$, clearly indicating the localization of all single-particle eigenstates, except for possibly a subset of zero measure; we find a similar result for all strengths of the potential we investigated. Still a non-extensive number of extended eigenstates, not captured by this analysis, is in principle sufficient to suppress localization *e.g.* in transport experiments⁴⁵, so that further analysis is required to complete the picture on the localization

properties of the frozen-boson potential (see Sec. V). The peak in the PR at the center of the band can be understood by the fact that the corresponding states have dominant $k = \pm\pi/2$ components, which are also the dominant Fourier components of the random potential for half filling.

We now move on to discuss the properties of the *many-body* ground state for hardcore bosons in the frozen-boson potential. Making contact with the discussion of Sec. II A, such a ground state can be reached by adiabatically turning on the interaction W between the two species after having prepared each of them separately and having quenched the hopping of the frozen bosons. In particular we analyze the properties of the disorder-averaged OPDM, which is translationally invariant, so that its eigenvalues correspond to the momentum distribution function (MDF), and hence average condensation properties are studied in momentum space through the scaling of $\lambda_0 = n_{k=0}$ with the number of particles N .

The scaling analysis of the disorder-averaged occupations of the lowest natural orbitals λ_0 is shown in Fig. 2 where, as N grows, N^f and L are grown correspondingly such that $N = N^f = L/2$. For small system sizes the hardcore bosons show quasi-condensation behaviour $\lambda_0 \sim N^\alpha$, with $\alpha = 0.5$ within the error given by the simulation, but for larger system sizes λ_0 saturates, hence revealing the absence of quasi-condensation in the thermodynamic limit. As shown in Fig. 2, the same quantity for the potential generated by fully uncorrelated frozen particles gives a completely analogous picture. This crossover can be qualitatively explained as a fragmentation effect. The lowest natural orbital in each disorder configuration is localized, namely it does not scale with the system size and hence it can only accommodate a finite number of particles, since the bosons repel each other.

As translational invariance is restored after disorder-averaging, the eigenvalues of the disorder-averaged OPDM correspond to the momentum distribution function. The peak at zero momentum, in which quasi-condensation appears in the case without disorder, is significantly reduced in presence of disorder. A scaling analysis of $n_{k=0}$ of the mobile bosons, shown in Fig. 2 detects a similar crossover from algebraic increase to saturation as for the disorder-averaged λ_0 . Therefore, the consequences of fragmentation extends to this experimentally accessible observable, and we can conclude on the absence of quasi-condensation in the disorder-averaged OPDM of the ground state of the system⁴². Moreover the density of states, shown in the lower panel of Fig. 1, reveals a continuous excitation spectrum at all energies. Hence, for a system of interacting bosons, the absence of quasi-condensation, together with the absence of gaps in the density of states, leads to classify the state of the system as a *Bose glass*. At the same time the Jordan-Wigner transformation translates this phase into an ideal Anderson insulator of non-interacting fermions.

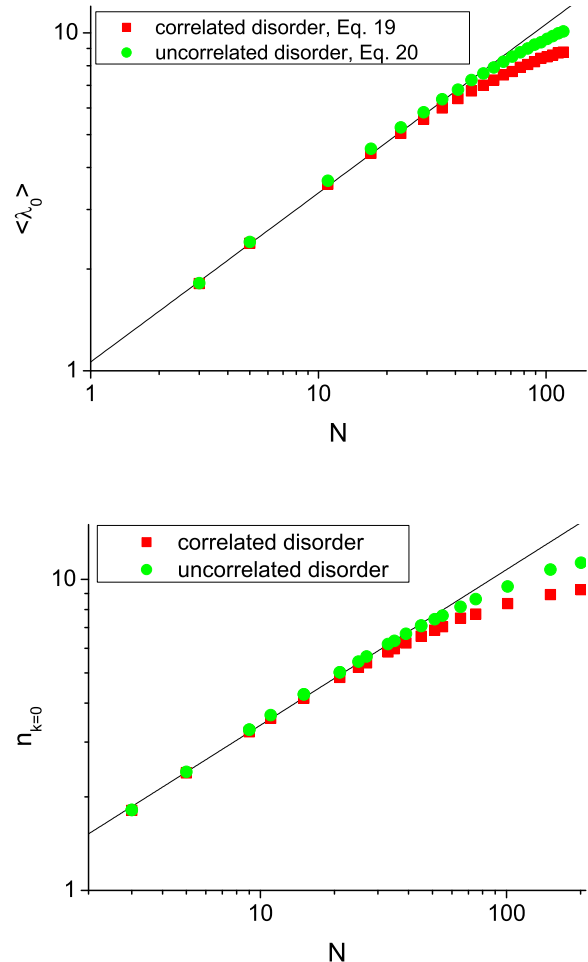


FIG. 2: (Color online) Scaling of the disorder-averaged largest eigenvalue λ_0 of the OPDM (upper plot) and the occupation of the zero momentum state $n_{k=0}$ (lower plot) for the ground state of a half-filled system of mobile bosons, interacting with the disorder potential. The cases of a correlated potential resulting from the superfluid state, Eq. (19), and that of a fully uncorrelated potential, Eq. (20), are compared. Here the strength of disorder is $W = 0.5J$. The black lines are fits to $n_{k=0}, \langle \lambda_0 \rangle \propto \sqrt{N}$ for the first four data points.

IV. DYNAMICAL PROPERTIES AFTER SUDDEN ON-TURN OF THE DISORDER POTENTIAL

While the previous section investigated the state of the mobile bosons after an adiabatic on-turn of the interaction with the disorder potential created by the frozen bosons, in this section we consider the evolution of the mobile bosons after turning on that interaction suddenly. We consider such a time evolution in the homogeneous system, *i.e.* $V = V^f = 0$, with periodic boundary conditions, mimicking the situation in which both species

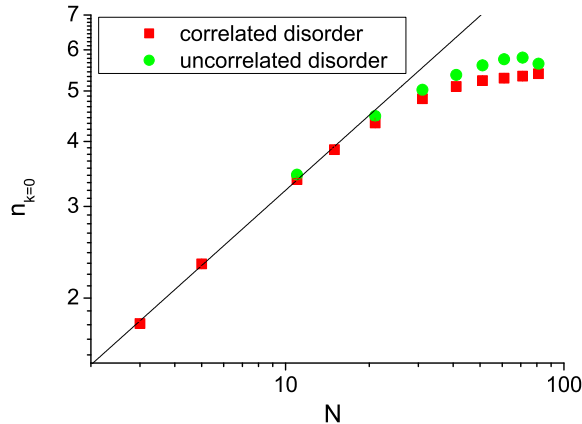


FIG. 3: (Color online) Scaling of the steady-state zero-momentum occupation $n_{k=0}$ with the particle number N in a homogeneous system of mobile and frozen bosons ($V = V^f = 0$) at half-filling ($N = N^f = L/2$), with interaction strength $W = 0.5J$. The line corresponds to a fit $n_{k=0} \sim \sqrt{N}$ to the first four data points.

of particles are prepared in the same region of space before being brought into interaction. In this situation, the disorder-averaged real-space density of the mobile bosons remains uniform during time evolution, so that real-space localization effects are not visible. Nonetheless, even in a more realistic experimental scenario, in which both species of particles are kept in the same nonvanishing trap ($V = V^f > 0$), the disorder-averaged density profile of the mobile species does not reveal marked localization effects, and it is even expanding during time evolution in order to reduce the overlap with the confined frozen bosons^{28,44}.

The fundamental effect of disorder on the time evolution can be very clearly detected in momentum space, which can be measured in time-of-flight experiments. The initial quasi-condensation peak in the MDF at $k = 0$ decreases quickly during time evolution until a stationary regime is reached, in which the value of $n_{k=0}$ is oscillating with a small amplitude ($\sim 1\%$). The scaling analysis for the value of $n_{k=0}$, time-averaged over the small oscillations, is shown in Fig. 3 for a half-filled system of mobile bosons. The occupation of the zero momentum state $n_{k=0}$ increases approximately like \sqrt{N} for small N , but it then deviates from an algebraic increase and saturates for larger N ; a completely analogous behavior is found for the case of uncorrelated disorder. Hence the scaling of $n_{k=0}$ reveals a crossover from quasi-condensation to fragmentation, with close similarity to the case of adiabatic evolution described in Sec. III; in analogy to that case, we conclude that the steady state reached by time evolution realizes *dynamically* a Bose glass.

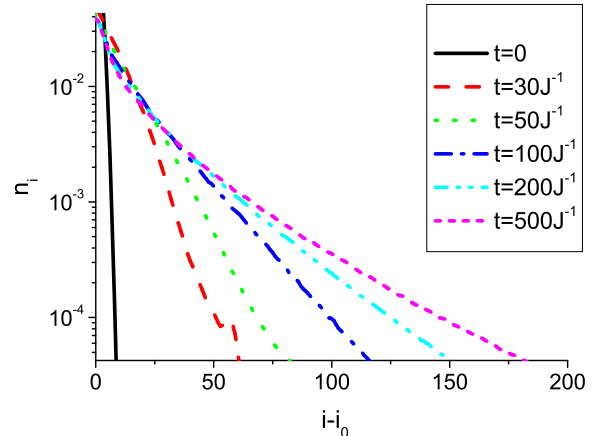


FIG. 4: (Color online) Snapshot of the evolution of the real-space density n_i for a single particle, initially in the ground state of a harmonic trap with $V = 0.01J$, and interacting with a correlated disorder potential. Here the interaction strength is $W = 0.5J$, and the system size is $L = 502$.

V. TRANSPORT PROPERTIES

In this section we discuss the expansion properties of initially confined mobile bosons in the potential created by the frozen particles. The initial confinement for the mobile particles is provided by a tight parabolic trap ($V > 0$), while the frozen particles can be imagined as prepared in a much shallower trap, whose effect is ignored for simplicity, so that the random potential they generate is the same as the one studied in the homogeneous case in Sec. IID. In particular we imagine that at time $t = 0$ the trap confining the mobile bosons is released ($V = 0$) and simultaneously the two species are brought into interaction ($W > 0$). After release from the trap, the mobile particles would expand forever in absence of disorder, so that a halt in presence of disorder explicitly shows localization effects.

Subsection VA deals with the evolution of the real-space properties during expansion, while Subsection VB studies the evolution of the condensation properties of the system.

A. Real-space localization

In this subsection we focus on the real-space properties of the time-evolved hardcore bosons in the frozen-boson potential, starting from a confined state in a parabolic trap. Snapshots from a disorder-averaged time evolution of a *single* particle starting from the ground state in the trap are depicted in Fig. 4. It is shown that the expansion reaches a *localized* steady state in the long-time limit; in particular the spatial decay of the particle density under-

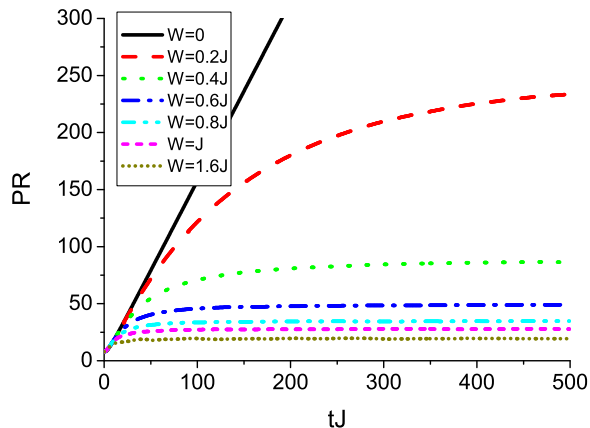


FIG. 5: (Color online) Time evolution of the participation ratio of a single particle for various disorder strengths. Other parameters as in Fig. 4.

goes a dramatic change from *Gaussian* - as expected in a parabolic trap - to *exponential* - as expected in presence of Anderson localization. Hence an Anderson localized state is realized dynamically during expansion; it is fundamental to stress that this steady state does not correspond to the ground state of the system, as the energy of the particle is conserved during expansion and hence it does not relax to the ground-state value.

The dynamical localization of the single particle wavefunction is fully captured by the time evolution of the PR, depicted in Fig. 5 for various strengths W of the disorder potential. Without disorder, the wavefunction spreads ballistically without changing its Gaussian shape³⁶. In the presence of disorder, the PR saturates instead to a finite value, which decreases when increasing the disorder potential; a fit to the final value of the PR, shown in Fig. 6, suggests that saturation in the PR takes place for any arbitrarily small value of the potential, as it would be expected for uncorrelated disorder, although exploring very small strengths of the disorder is numerically demanding as the steady state is reached for prohibitively large values of the PR.

The time evolution of the participation ratio of many particles initially confined in a harmonic trap is similar to that exhibited by a single particle, and a saturation of the PR to a steady-state value is observed for the smallest value of W that we could treat numerically (Fig. 6).

Nonetheless, upon increasing the particle number in the trap beyond a critical value $N_c \approx 26$ (see equation 14 with $V = 0.01$) a Mott plateau at unit filling starts forming in the center, and the properties of the initial trapped ground state change drastically. It is then interesting to study whether the different initial conditions for

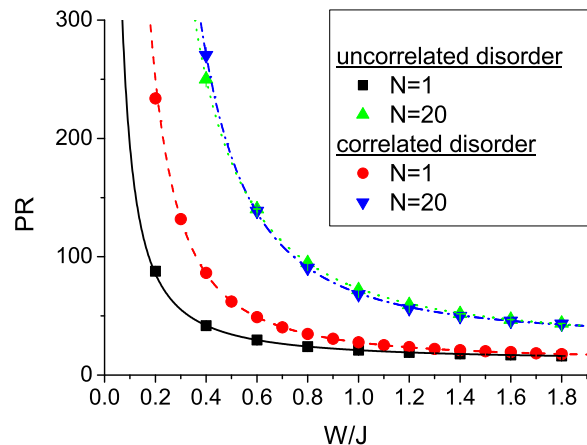


FIG. 6: (Color online) Steady state participation ratio (recorded at $t = 500J^{-1}$) for N particles, time-evolved in a system of size $L = 702$ starting from the ground state of a harmonic trap ($V = 0.01J$) and interacting with a correlated random potential or with a fully uncorrelated random potential. The lines show a fit to the data points with an algebraically decaying function.

the time evolution reflect themselves in the steady state of the system after the halt of the expansion. The upper plot of Fig. 7 shows the PR of the steady state as a function of the number of particles N . The steady state PR increases with the number of particles for $N \leq N_c$, showing a small peak for $N = N_c$ beyond which the increase with N is much slower. This feature can be understood in terms of the time evolution of the fermionic wavefunction Eq. (11), whose real-space properties such as the PR are equivalent to those of the hardcore bosons, and whose time evolution is simply obtained through the time evolution of single-particle eigenfunctions. For $N > N_c$ the single particle wavefunctions that are populated for increasing N are more and more confined to the sides of the trap, as the center has already a saturated density, and their energy is dominated by the trapping term, while the single-particle kinetic energy *decreases* with increasing N beyond N_c (see lower plot of Fig. 7). Given that the trapping energy vanishes at $t = 0$ after the trap release, the fermions occupying levels beyond the N_c -th expand with an energy which is less than that of the N_c -th level, so that they are expected to be localized by the disorder potential with a final participation ratio which is similar (or even less than) that of the N_c -th particle. The time-evolved particle density of the many-body system is the simple sum of the squared time-evolved wavefunctions of the free fermions, so that the total participation ratio is not expected to increase significantly when adding particles beyond the N_c -th.

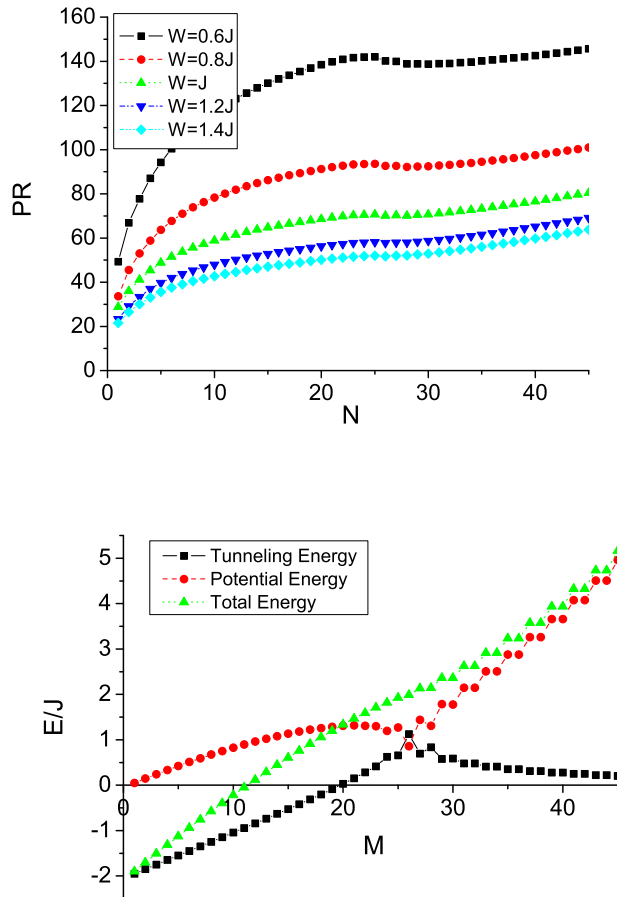


FIG. 7: (Color online) Upper plot: Steady-state participation ratio (recorded at $t = 400J^{-1}$) of N particles as a function of the particle number for various disorder strengths. Other parameters as in Fig. 6. Lower plot: Total, kinetic, and potential energy of the M th single-particle eigenstate of the initial system in the trap.

B. Coherence properties

In the previous section the real-space properties of initially confined hardcore bosons expanding in a disorder potential have been discussed. This section addresses the condensation properties of the same system, motivated by the rich physical scenario offered by expanding hardcore bosons in absence of disorder^{36,37}. Subsection VB 1 is devoted to the time evolution of hardcore bosons initially confined in a superfluid state, while Subsection VB 2 analyses the expansion from a Mott insulator.

1. Time evolution starting from a superfluid state

This subsection focuses on the expansion of the hardcore bosons initially confined in a shallow trap with char-

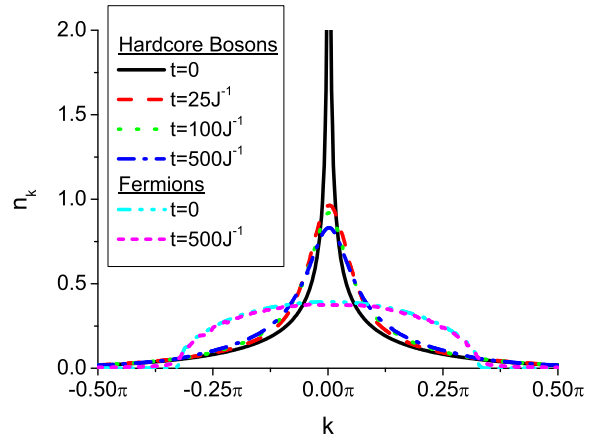


FIG. 8: (Color online) Snapshots of the time evolution of the momentum distribution n_k for a system of $N = 100$ hardcore bosons, initially in a trap with density $\bar{\rho} = 0.5$, interacting with a correlated disorder potential. Here the system size is $L = 1002$ and the interaction strength is $W = 0.5J$. The momentum distribution for the corresponding spinless fermions is shown for comparison.

acteristic density $\bar{\rho} = 0.5$ (see Eq. (14)) well below the critical value $\bar{\rho}_c \approx 2.6$ for the onset of a Mott plateau in the trap center. With this initial condition quasi-condensation in the first NO is present, and the MDF is peaked around $k = 0$ at $t = 0$ ³⁷. In the absence of disorder the MDF evolves towards that of the fermions (which is a constant of motion), namely the bosons *fermionize* in momentum space, although they still quasi-condense in the lowest NO which contains many momentum components³⁷. Furthermore, the OPDM is decaying algebraically like $\rho_{i,i+r} \sim |r|^{-0.5}$, showing quasi-long-range order, whereas the phase of the OPDM is oscillating at large distances leading to fermionization in momentum space. The decay of the OPDM is measured from the center of the trap, i.e. the center of the lowest NO and the site with maximum occupation.

We now move on to the analysis of the evolution of the MDF during expansion from a shallow trap in the presence of disorder created by the frozen bosons. The MDF of the mobile hardcore bosons is depicted in Fig. 8 at different times t , compared to the MDF of fermions in the same system. In presence of disorder the MDF of the fermions is no longer a constant of motion, but it is only slightly broadening in time due to its interaction with the frozen species of particles. The effect of the disorder potential on the hardcore bosons is more significant. The $t = 0$ peak at zero momentum reduces its height, but, contrary to the expansion without disorder, it does not disappear and fermionization is not present. Following Ref. 37, fermionization in absence of disorder is understood through the argument that, after

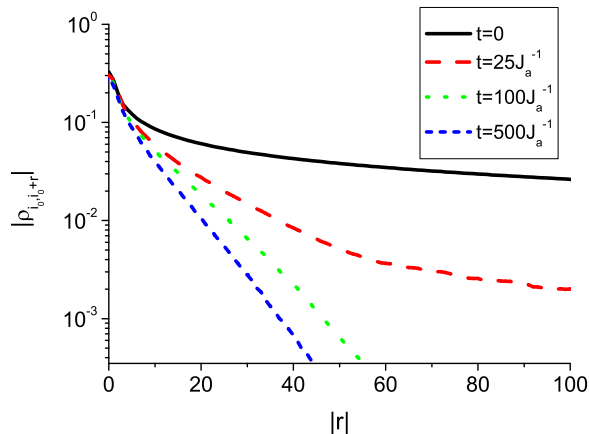


FIG. 9: (Color online) Decay of the modulus of the OPDM $|\rho_{i_0, i_0+r}|$ from the system center i_0 at various times during evolution. Parameters as in Fig. 8.

a long-term expansion, the hardcore-boson system is dilute enough to be considered essentially non-interacting, and so it becomes equivalent to its fermionic counterpart. In presence of disorder, on the contrary, the expansion is stopped by localization, so that the extremely dilute limit is never reached and the hardcore bosons preserve their nature of strongly interacting particles. Furthermore, the interaction with a disorder potential leads to the loss of quasi-long-range order during time evolution, as shown in Fig. 9 by the decay of the OPDM at various times. The system finally reaches a steady state with an exponentially decaying OPDM.

The loss of quasi-long-range order during expansion strongly suggests the loss of quasi-condensation in the system. As the initial conditions break the translational symmetry, condensation properties are not captured by the scaling of the occupation of the zero-momentum state, and direct diagonalization of the disorder-averaged OPDM is necessary to extract the scaling of the occupation λ_0 of the lowest natural orbital. λ_0 decreases during time evolution, reaching a constant value in correspondence with the steady state observed in real-space. The scaling analysis of λ_0 is performed for this constant value in Fig. 10. The scaling of λ_0 deviates from the quasi-condensation behavior at sufficiently large particle numbers, revealing a crossover from quasi-condensation to fragmentation due to the localized nature of the lowest NO. Fully uncorrelated disorder leads to a similar behavior, although the crossover appears to be much broader, and a quasi-condensation regime at low N could not be identified.

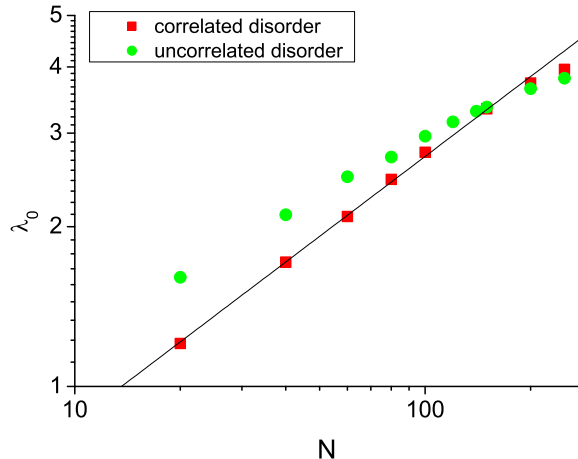


FIG. 10: (Color online) Scaling of the steady-state λ_0 (recorded at time $t = 500J^{-1}$) for varying number of particles in a system of size $L = 1502$; other parameters as in Fig. 8. The data for correlated frozen bosons are compared with those for fully uncorrelated ones. The line corresponds to a fit to $\lambda_0 \sim \sqrt{N}$.

2. Time Evolution starting from a Mott insulator

As reported in Ref. 36, hardcore bosons prepared in a perfect Mott insulating state (corresponding to an infinitely steep trap) and subsequently time evolved exhibit the phenomenon of dynamical quasi-condensation at finite momentum. Indeed, from the initially flat MDF of the Mott insulator two quasi-condensation peaks emerge at momenta $k = \pm\pi/2$ during time evolution³⁶, as reproduced in Fig. 11. Strictly speaking quasi-condensation happens in two degenerate NOs whose Fourier transform is sharply peaked around $k = \pm\pi/2$; the NOs propagate at a velocity $v = \pm 2J$ corresponding to the maximal group velocities $\partial\epsilon_k/\partial k$ for the single-particle dispersion relation $\epsilon_k = -2J \cos k$ at momenta $k = \pm\pi/2$.

The occupation of the degenerate lowest NOs, λ_0 , follows initially a universal power-law increase with time, independent of the number of particles N ; at an N -dependent characteristic time τ_c , the two degenerate lowest NOs begin to move in opposite directions, and λ_0 starts to algebraically decrease, although its scaling with particle number shows the typical quasi-condensation behavior $\lambda_0 \sim \sqrt{N}$. The two lowest NOs clearly appear in the real-space densities as coherent fronts of the atomic cloud moving in opposite directions (see Fig. 11). This aspect suggests the use of this setup to produce an atom laser³⁶.

We now consider the case of expanding hardcore bosons in the disorder potential created by frozen particles. Fig. 12 shows the density profile and the MDF for the expansion from a perfect Mott insulator in the

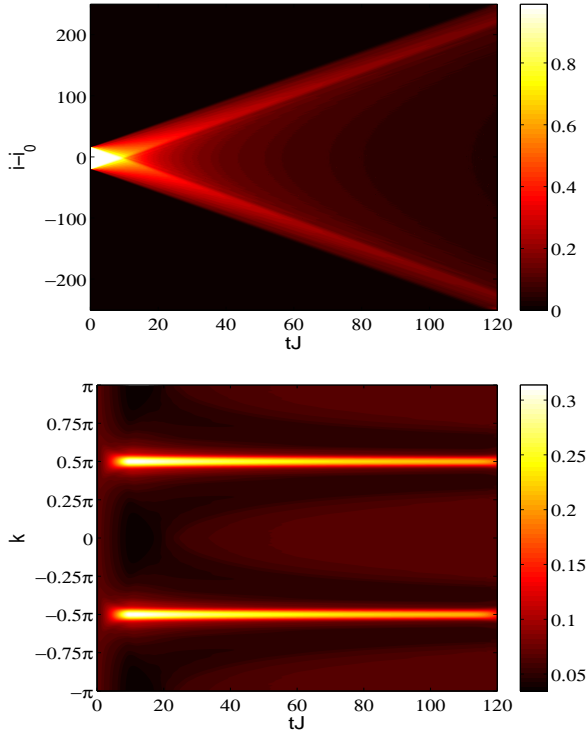


FIG. 11: (Color online) Time evolution of the density profile (upper image) and the momentum distribution function (lower image) of $N = 35$ hardcore bosons, initially in a perfect Mott insulator, in a system of size $L = 502$ without disorder.

presence of disorder created by frozen particles. Initially peaks at momenta $k = \pm\pi/2$ are emerging from the flat MDF at $t = 0$ as in the case without disorder, and the hardcore boson cloud shows two outer fronts expanding ballistically in opposite directions. Nonetheless this initially coherent expansion is rapidly suppressed due to localization, which leads to a decrease and broadening of the momentum peaks at larger times up to a final steady-state MDF in which two broad peaks survive, and which corresponds to a localized state in real space as seen in Subsection V A.

A deeper analysis of condensation effects relies on the NOs and their occupations. Figs. 13 and 14 show the time evolution of the largest eigenvalue λ_0 for different disorder strengths and different particle numbers. Initially λ_0 is two-fold degenerate, corresponding to reflection symmetry at the center of the system, and it increases following a universal power law independent of the particle number, similarly to what is observed in absence of disorder but with a different disorder-dependent exponent. As in the case $W = 0$, at a characteristic time τ_c the two degenerate natural orbitals start to move into opposite directions, and correspondingly the time evolution of λ_0 turns into a decreasing behavior; τ_c strongly depends on the disorder strength (Fig. 13), while its dependence on the particle number N becomes weaker for

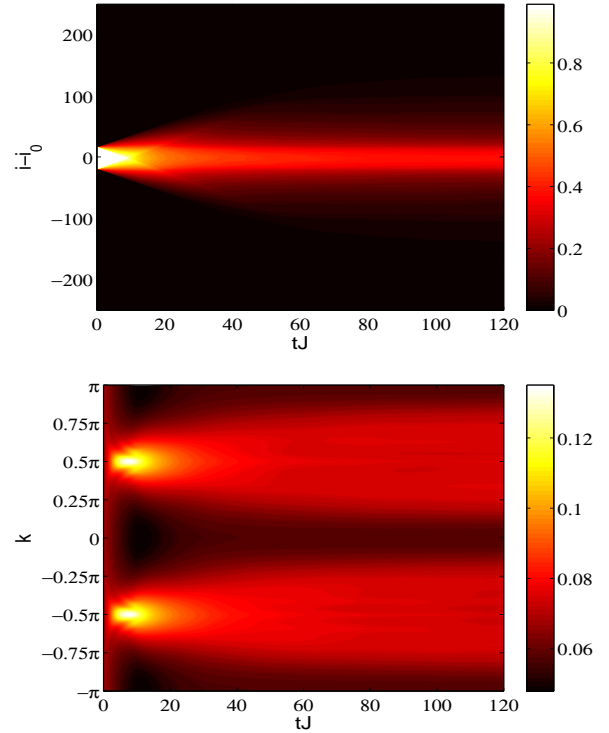


FIG. 12: (Color online) Time evolution of the density profile (upper image) and the momentum distribution function (lower image) of $N = 35$ hardcore bosons, initially in a Mott insulator, interacting with the disorder potential created by frozen particles at half-filling. Here the interaction strength is $W = 0.5J$.

large N , where τ_c is seen to approach an asymptotic value (Fig. 14). Unlike the case $W = 0$, at a later stage the expansion of the system is stopped by disorder, and the degeneracy in the lowest NOs is removed, going from two propagating ones to a single NO localized in the system center.

Hence the expanding system of hardcore bosons from a pure Mott state shows a crossover from an incipient quasi-condensation regime at finite momenta to a localization regime. It is natural to ask whether the system displays true quasi-condensation at any intermediate point in time. To address this issue, we perform a scaling analysis of λ_0 at the maximum-coherence time $t = \tau_c$. The results of this analysis are shown in Fig. 15, where λ_0 exhibits a clear saturation for large particle numbers, and hence a crossover from quasi-condensation to fragmentation. Repeating the same analysis for uncorrelated random disorder we find a scaling of λ_0 which is in qualitative agreement with the case of disorder generated by frozen particles (the apparent quantitative agreement is accidental).

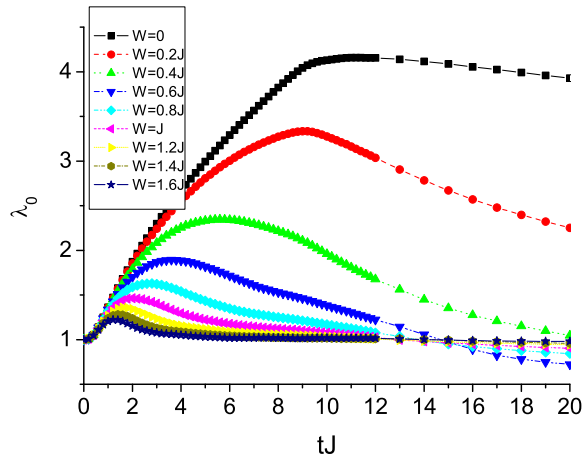


FIG. 13: (Color online) Time evolution of λ_0 for various disorder strengths. Other parameters as in Fig. 12.

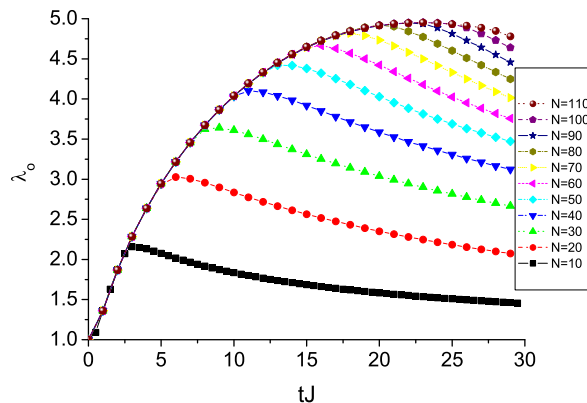


FIG. 14: (Color online) Time evolution of λ_0 for various numbers of particles, and for disorder strength $W = 0.1J$. Other parameters as in Fig. 12.

VI. EXPERIMENTAL REALIZATION

The original experimental proposal motivating this work is reported in Ref. 28, where the use of state-dependent lattices was initially envisioned to create the quantum superposition of random potentials. As shown in Ref. 31, two hyperfine states of the same atomic species can be loaded in the minima of two different polarization components of an optical lattice at a so called "magic wavelength"^{5,29,30}, at which each hyperfine state couples to one and only one polarization component. Hence, if the two polarization components are initially shifted by $\pi/2$ in space, the two species are non essentially interacting (see Fig. 16). The possibility of increasing dras-

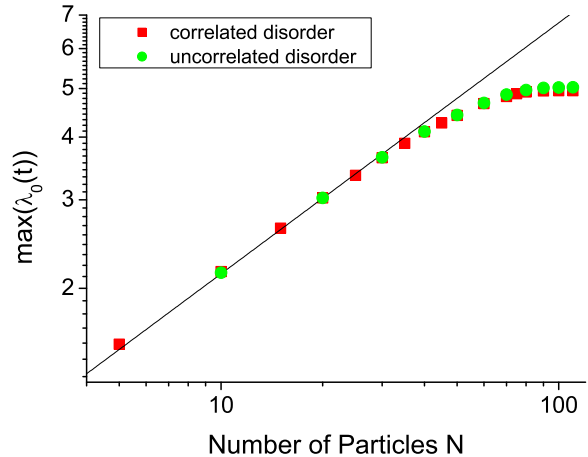


FIG. 15: (Color online) Scaling of the maximal value of λ_0 during time evolution of N hardcore bosons, initially in a Mott insulator. All parameters as in Fig. 14. The line corresponds to a fit to $\lambda_0 \sim \sqrt{N}$ of the first four data points.

tically the intensity of one of the two polarization components would allow for a sudden quench of the hopping of one of the two species, preparing in this way the quantum superposition of random potentials. The two species can be then brought into interaction at different strengths by shifting the spatial phase between the two polarization components of the lattice. An adiabatic shift would transfer the mobile species to the Bose-glass ground state in the random potential, as discussed in Section III, whereas a sudden shift would give rise to an out-of-equilibrium Bose-glass state as steady state after a transient evolution, as discussed in Section IV. As demonstrated in Ref. 33, the hardcore regime is achieved by using deep lattices for both polarization components and extremely dilute gases of both hyperfine states, so that a density of less than one atom per site is achieved in the lattice after loading.

As seen in Section V, expansion experiments in the disorder potential require to confine the two components with strongly different trapping frequencies, and then to release one of the two traps independently of the other. Making use of the selective coupling of different hyperfine states to different polarization components of a magic-wavelength laser, it is possible to more strongly confine one of the two species through an optical dipole trap obtained by a tightly focused and polarized laser propagating transverse to the chain direction in the one-dimensional optical lattice.

Throughout all the previous Sections we have seen that the onset of localization leaves very strong signatures on the momentum distribution, which is observed in standard time-of-flight experiments. Moreover expansion experiments in the disorder potential lead to exponen-

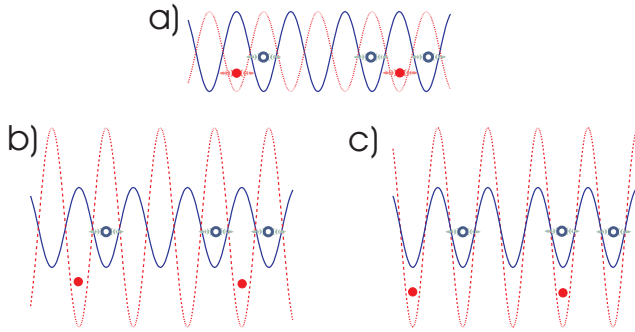


FIG. 16: (Color online) Sketch of the preparation of the disorder potential and of the tuning of its strength using state-dependent optical lattices for a mixture of atoms in two internal states. The two species are first prepared in two shifted optical lattices (a), then one of the two optical lattices is increased in strength so as to freeze one of the two bosonic species (b), and finally the spatial phase of the two lattices is changed to bring the two species into interaction (c).

tially localized steady states, whose density profile can be reconstructed by absorption images taken shortly after turning off all lasers^{7,8,9,10}. Despite the averaging over the various tubes of the one-dimensional optical lattice³³, the extreme tails of the averaged particle density distribution should be dominated by the exponentially localized tails of the particle density in the central tubes of the one-dimensional optical lattice.

VII. CONCLUSIONS

In this paper we have shown that a gas of one-dimensional hardcore bosons undergoes genuine quantum localization effects when set into interaction with a secondary species of bosons frozen in a massive quantum superposition of Fock states. Each Fock state can be regarded as a realization of a random potential, and the unitary evolution of the mobile species of bosons follows all possible paths related to the various disorder realizations *in parallel*. Physically relevant states in which one

can prepare the frozen bosons, as for instance the superfluid state in the hardcore limit, realize a rapidly fluctuating disorder potential over the length scale of a few lattice spacings; despite its power-law decaying correlations, the disorder potential is found to lead to the same localization effects as those observed in a *fully uncorrelated* potential. In the hardcore boson limit for the mobile species these effects can be studied exactly in real time through Jordan-Wigner diagonalization, and we can numerically simulate realistic experimental setups for the dynamical preparation of localized many-body states. The equilibrium state of the hardcore bosons in the random potential is found to be a homogeneous Bose-glass state with exponentially decaying correlations; a similar state can be realized also dynamically after a sudden on-turn of the interaction between the two species. When the hardcore bosons are initially confined in a tight trap and then set free to expand in the random potential, for any non-vanishing disorder strengths the expansion stops and the system reaches an exponentially localized state.

For any setup discussed in this work, we observe the absence of quasi-condensation and quasi-long-range order due to the disorder potential. When the two species are confined in the same region and brought into interaction, the steady state of the system displays exponentially decaying off-diagonal correlations; in the expansion experiments the disorder potential destroys the effects of fermionization (when expanding from an initially dilute state) and quasi-condensation at finite momentum (when expanding from a Mott state). Hence disorder created by a species of frozen hardcore bosons represents a very robust way to experimentally implement strongly fluctuating random potentials in optical lattices, and to realize fundamental localization effects of many-body systems.

VIII. ACKNOWLEDGEMENTS

We thank J. J. García-Ripoll and V. Murg for useful discussions. This work is supported by the European Union through the SCALA integrated Project.

¹ D. Jaksch, C. Bruder, J.I. Cirac, C.W. Gardiner, and P. Zoller, Phys. Rev. Lett. **81**, 3108 (1998).

² M. Greiner, O. Mandel, T. Esslinger, T.W. Hänsch, and I. Bloch, Nature (London) **415**, 39 (2002).

³ I. Bloch, J. Dalibard, and W. Zwerger, cond-mat/0704.3011.

⁴ M. Lewenstein, A. Sanpera, V. Ahufinger, B. Damski, A. Sen De, and U. Sen, Advances in Physics **56**(2), 243 (2007).

⁵ D. Jaksch and P. Zoller, Annals of Physics **315**, 1 (2004).

⁶ E. Jané, G. Vidal, W. Dür, P. Zoller, and J.I. Cirac, Quant. Inform. Comput. **3**, 15 (2003).

⁷ J.E. Lye, L. Fallani, M. Modugno, D.S. Wiersma, C. Fort, and M. Inguscio, Phys. Rev. Lett. **95**, 070401 (2005).

⁸ D. Clément, A.F. Varón, M. Hugbart, J.A. Retter, P. Bouyer, L. Sanchez-Palencia, D.M. Gangardt, G.V. Shlyapnikov, and A. Aspect, Phys. Rev. Lett. **95**, 170409 (2005).

⁹ C. Fort, L. Fallani, V. Guarrera, J.E. Lye, M. Modugno, D.S. Wiersma, and M. Inguscio, Phys. Rev. Lett. **95**, 170410 (2005).

¹⁰ T. Schulte, S. Drenkelforth, J. Kruse, W. Ertmer, J. Arlt, K. Sacha, J. Zakrzewski, and M. Lewenstein, Phys. Rev. Lett. **95**, 170411 (2005).

¹¹ L. Fallani, J. E. Lye, V. Guarrera, C. Fort, and M. Inguscio, Phys. Rev. Lett. **98**, 130404 (2007).

¹² T. Schulte, S. Drenkelforth, J. Kruse, R. Tiemeyer, K.

- Sacha, J. Zakrzewski, M. Lewenstein, W. Ertmer, and J.J. Arlt, *New J. Phys.* **8**, 230 (2006).
- ¹³ R. Roth and K. Burnett, *J. Opt. B* **5**, S50 (2003).
- ¹⁴ R. Roth and K. Burnett, *Phys. Rev. A* **68**, 023604 (2003).
- ¹⁵ B. Damski, J. Zakrzewski, L. Santos, P. Zoller, and M. Lewenstein, *Phys. Rev. Lett.* **91**, 080403 (2003).
- ¹⁶ R.C. Kuhn, C. Miniatura, D. Delande, O. Sigwarth, and C.A. Müller, *Phys. Rev. Lett.* **95**, 250403 (2005).
- ¹⁷ L. Sanchez-Palencia, D. Clément, P. Lugan, P. Bouyer, G.V. Shlyapnikov, and A. Aspect, *Phys. Rev. Lett.* **98**, 210401 (2007).
- ¹⁸ D. Clément, A.F. Varón, J.A. Retter, L. Sanchez-Palencia, A. Aspect, and P. Bouyer, *New Journal of Physics* **8**, 165 (2006).
- ¹⁹ P. Lugan, D. Clément, P. Bouyer, A. Aspect, M. Lewenstein, and L. Sanchez-Palencia, *Phys. Rev. Lett* **98**, 170403 (2007).
- ²⁰ L. Sanchez-Palencia, *Phys. Rev. A* **74**, 053625 (2006).
- ²¹ H. Gimperlein, S. Wessel, J. Schmiedmayer, and L. Santos *Phys. Rev. Lett.* **95**, 170401 (2005).
- ²² P. Sengupta, A. Raghavan, and S. Haas *New J. Phys.* **9**, 103 (2007).
- ²³ A. Sanpera, A. Kantian, L. Sanchez-Palencia, J. Zakrzewski, and M. Lewenstein, *Phys. Rev. Lett* **93**, 4 (2004).
- ²⁴ M.P.A. Fisher, P.B. Weichman, G. Grinstein, and D.S. Fisher, *Phys. Rev. B* **40**, 546 (1989).
- ²⁵ Nevertheless, recent theoretical works has shown that laser-speckle potentials within experimental reach can possibly lead to Anderson localization of weakly interacting bosons^{16,17,18,19}.
- ²⁶ A. M. Rey, I. I. Satija, and C. W. Clark, *Phys. Rev. A* **73**, 063610 (2006).
- ²⁷ U. Gavish and Y. Castin, *Phys. Rev. Lett.* **95**, 020401 (2005).
- ²⁸ B. Paredes, F. Verstraete, and J.I. Cirac, *Phys. Rev. Lett.* **95**, 140501 (2005).
- ²⁹ D. Jaksch, H.-J. Briegel, J.I. Cirac, C.W. Gardiner, and P. Zoller, *Phys. Rev. Lett.* **82**, 1975 (1999).
- ³⁰ G.K. Brennen, C.M. Caves, P.S. Jessen, and I.H. Deutsch, *Phys. Rev. Lett.* **82**, 1060 (1999).
- ³¹ O. Mandel, M. Greiner, A. Widera, T. Rom, T.W. Hänsch, and I. Bloch, *Nature* **425**, 937 (2003).
- ³² E. Lieb, Schultz, and D. Mattis, *Ann. Phys. (NY)* **16**, 406 (1961).
- ³³ B. Paredes, A. Widera, V. Murg, O. Mandel, S. Fölling, I.J. Cirac, G.V. Shlyapnikov, T.W. Hänsch, and I. Bloch, *Nature* **429**, 277 (2004).
- ³⁴ T. Kinoshita, T.R. Wenger, and D.S. Weiss, *Science* **305**, 1125 (2004).
- ³⁵ M. Rigol and A. Muramatsu, *Phys. Rev. A* **70**, 031603(R) (2004); M. Rigol and A. Muramatsu, *Phys. Rev. A* **72**, 013604 (2005).
- ³⁶ M. Rigol and A. Muramatsu, *Phys. Rev. Lett.* **93**, 230404 (2004).
- ³⁷ M. Rigol and A. Muramatsu, *Phys. Rev. Lett.* **94**, 240403 (2005).
- ³⁸ E. Abrahams, P.W. Anderson, D.C. Licciardello, T.V. Ramakrishnan, *Phys. Rev. Lett.* **42**, 673 (1979).
- ³⁹ K. Ishii, *Suppl. Progr. Theor. Phys.* **53**, 77 (1972); D. J. Thouless, *Phys. Rep.* **13**, 93 (1974).
- ⁴⁰ O. Penrose and L. Onsager, *Phys. Rev.* **104**, 576 (1956).
- ⁴¹ V.E. Korepin, A.G. Izergin, and N.M. Bogoliubov, *Quantum Inverse Scattering Method and Correlation Functions*, Cambridge University Press (1993).
- ⁴² Although the disorder-averaged largest eigenvalue $\langle \lambda_0 \rangle$ and the disorder-averaged $k = 0$ occupation $n_{k=0}$ show a similar scaling with system size, they have no simple relationship to each other; indeed λ_0 refers to localized natural orbitals, while $n_{k=0}$ is associated with an extended one.
- ⁴³ The uncorrelated frozen bosons are considered to be in the state $|\Phi^f\rangle = \otimes_{i=1}^L (1 + a_i^\dagger)|0\rangle$ projected on the subspace with a fixed number of particles. This state cannot straightforwardly be prepared in an optical lattice.
- ⁴⁴ B. Horstmann, Diploma Thesis, Friedrich-Schiller-Universität Jena (2007), unpublished.
- ⁴⁵ D.H. Dunlap, H.-L. Wu, P.W. Phillips, *Phys. Rev. Lett.* **65**, 88 (1990).